

Flight Performance of the BESS-Polar Aerogel Cherenkov Counter

T. Hams^{a*}, K. Abe^{b†}, H. Fuke^c, S. Haino^d, K.C. Kim^e, T. Kumazawa^d, M.H. Lee^e,
Y. Makida^d, S. Matsuda^f, H. Matsumoto^f, K. Matsumoto^d, J.W. Mitchell^a, A.A. Moiseev^a,
Z.D. Myers^e, J. Nishimura^f, M. Nozaki^b, A. Ogata^b, M. Oikawa^b, J.F. Ormes^a, M. Sasaki^{a*},
E.S. Seo^e, Y. Shikaze^{b‡}, R.E. Streitmatter^a, J. Suzuki^d, K. Takeuchi^b, K. Tanaka^d,
T. Taniguchi^d, T. Yamagami^c, A. Yamamoto^d, T. Yoshida^d, K. Yoshimura^d

(a) NASA Goddard Space Flight Center (NASA/GSFC), Greenbelt, MD 20771 USA

(b) Kobe University, Kobe, Hyogo, 657-8501, Japan

(c) Institute of Space and Astronautical Science (ISAS/JAXA), Sagami-hara, Kanagawa, 229-8510 Japan

(d) High Energy Accelerator Research Organization (KEK), Tsukuba, Ibaraki, 305-0801 Japan

(e) University of Maryland, College Park, MD 20742 USA

(f) The University of Tokyo, Bunkyo, Tokyo, 113-0033 Japan

Presenter: Thomas Hams (hams@milkyway.gsfc.nasa.gov), usa-hams-T-abs1-og11-oral

The BESS-Polar balloon payload had its first flight on December 13th-21st, 2004 (UTC) from McMurdo Station, Antarctica. The flight duration was over eight days and more than 9×10^8 cosmic-ray events were recorded. An overview of the BESS-Polar flight, the status of the antiproton analysis, and a discussion of the low-power readout electronics and data acquisition system can be found elsewhere in these proceedings. In this paper we discuss the design, testing, and flight performance of the BESS-Polar Cherenkov counter, which operated in ambient conditions outside a pressure vessel. The silica-aerogel Cherenkov radiator had a nominal index-of-refraction, $n = 1.02$, yielding an lower limit for the most likely photoelectron (PE) number of 7 in the center of the counter and 9 near the photomultiplier tubes.

1. Introduction

BESS-Polar is a new balloon payload and is a successor instrument in the ongoing BESS (Balloon-borne Experiment with a Superconducting Spectrometer) Program. A major scientific objective of BESS is the antimatter search. To identify incident cosmic radiation, the BESS-Polar instrument is equipped with a magnetic rigidity spectrometer consisting of a jet-type drift chamber surrounded by two layers of inner drift chamber inside the field of a superconducting solenoid magnet. A time-of-flight (TOF) system provides the velocity and charge determination. Using the velocity vs. rigidity technique a particle of a given charge can be identified. To extend particle identification to higher energies an aerogel Cherenkov counter (ACC) is used as a threshold detector. A lighter particle at the same rigidity as a heavier one may already be above the Cherenkov threshold and produce a signal in the counter whereas the heavier particle is still below the threshold and has no signature in the ACC.

To reduce the energy where cosmic-ray antiprotons can unambiguously be identified, BESS-Polar, in contrast to its predecessors, is configured with a more-transparent, ultra-thin magnet, no pressure vessel, an additional middle TOF counter above the lower magnet wall, and the aerogel Cherenkov counter repositioned between the magnet and the lower TOF. More details on the instrument description and the scientific goals of BESS-Polar can be found elsewhere [1].

BESS-Polar was launched on December 13, 2004, from McMurdo Station, Antarctica. After a successful flight

* Resident Associate of the National Research Council, USA

† Present address: Kamioka Observatory, ICRR, The University of Tokyo, Kamioka-cho, Gifu 506-1205 Japan

‡ Present address: Tokai Research Establishment, Japan Atomic Energy Research Institute, Tokai, Ibaraki 391-1195 Japan

of 8 days and 17 hours, the instrument landed near Siple Dome ~ 400 miles from McMurdo. The instrument was recovered successfully. During the BESS-Polar flight 9×10^8 cosmic-ray events were recorded. For more detail on the BESS-Polar flight and the status of the data analysis see [2] in these proceedings.

2. PMT assembly and Counter Design

The BESS-Polar Cherenkov counter consists of a light-diffusion box containing silica-aerogel with a nominal index-of-refraction, $n = 1.02$. The Cherenkov light is viewed by 46 fine-mesh Hamamatsu R6504 PMTs. The Cherenkov counter is located below the lower magnet wall, conforming to the cylindrical symmetry of the magnet, and its fiducial volume nearly covers the aperture defined by the TOF system. To make BESS-Polar more transparent to low energy particles, the instrument has no outer pressure vessel and as a consequence the outer TOF and the Cherenkov counter are exposed the ambient flight conditions. This fact needed to be reflected in the design of the Cherenkov box and the PMT assemblies.



Figure 1. Hermetic PMT housing.

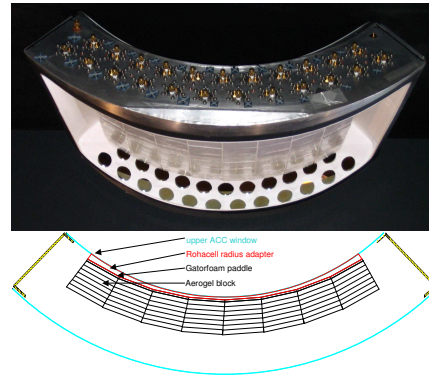


Figure 2. Photograph of ACC with lower window removed and cross section through the aerogel blocks.

To operate the ACC PMTs in a flight environment, Goddard developed a hermetic housing for each PMT. The housing was machined out of aluminum and had a outside diameter that was only ~ 4 mm larger than the nominal diameter of the 2.5-inch PMT and had a length of less than 89 mm, only 24 mm longer than the PMT. Fig. 1 shows the components of the hermetic PMT housing consisting of the tube-case, PMT with voltage-divider, Delrin cushion-ring, compression-nut, tube-base, connector-cap, and the counter light seal. The hermetic assembly with PMT weighs only 350 grams. The entrance window of the PMT is lightly pressed against an o-ring at the front lip of the tube-case. This lip is less than 1 mm thick and has an inner diameter that is greater than the active area (50 mm) of the photocathode. The pressure on the glass bulb of the PMT is exerted from the back by a compression-nut that screws into tube-case. A cushion-ring spreads the load across the beveled PMT rear-edge. The voltage-divider is designed such that it fits inside the cushion-ring and compression-nut. In addition, the Delrin cushion-ring provides an electric insulation between the voltage-divider and the tube-case. The back of the PMT housing is sealed by the tube-base and the connector-cap. The tube-base screws into the tube-case and is sealed by an o-ring. The tube-base also provides the interface to fasten the PMT housings to the mounting plate of the counter box. Signal- and HV-connectors on the PMT voltage-divider and inside of connector-cap, allow for easy installation of the connector-cap, which is held on the tube-base by screws. The tube-base together with a silicone-rubber gasket and the mounting plate is a light barrier and shields the inside of the counter from external light. When the PMT housing is installed in the counter, the connector-cap is protruding through a cut-out in the mounting plate (Fig. 2). The external bulkheads on the connector-cap are not only gas-tight but also light-tight and do not require external light

shielding. A Schrader valve on the connector-cap is used to evacuate the housing and backfill it with dry Nitrogen. Each PMT has a dedicated, programmable HV supply. PMT housing and HV supply use Series 600 connectors from Reynolds Industries. The nominal flight HV for the ACC PMTs was 1.7 kV (gain 7.5×10^6). Detail on the associated ACC PMT readout electronics can be found elsewhere in these proceedings [3].

The compact PMT housing allows the accommodation of 23 PMTs at each end of the counter (see Fig. 2). Due to the proximity of the ACC PMTs to the ends of the solenoid, the PMTs have to operate in a magnetic field of ~ 2000 Gauss. To align the PMTs axis to the local magnetic field the mounting plate is tilted at 31 degrees. The frame of cherenkov box is welded aluminum. To reduce the material in the path of the particle, upper and lower cover of the counter are 0.8 mm thick carbon fiber windows and cover the full TOF aperture. The windows are mounted with a light-tight seal onto the counter. A light-trap on either mounting plate allows the detector volume to reach ambient pressure. The light diffusion volume in the counter is lined with highly reflective Gore-Tex (0.25 mm). The reflector in front of the PMTs has almond-shaped cut-offs exposing only photocathode areas that are most efficient in the nearly axial magnetic field.

The silica-aerogel sheet used as a Cherenkov radiator is hydrophobic [4], has a nominal refractive index of $n = 1.02$, and a thickness of 11 mm. Fig. 2 shows a photo and cross section of the Cherenkov counter. Seven aerogel sheets are stacked to create an aerogel block, which have the dimension of 86.26 mm at the top, 97.51 mm at the bottom, and 92.7 mm along the axis of the magnet. The aerogel sheets were water-jet cut to create this one-sided tapered block. The layers in an aerogel block are held together by a highly UV-transparent plastic wrap. Nine aerogel blocks are placed along the axis of the magnet on 5 mm thick Gatorfoam paddle, a low-density laminated foam core composite. The blocks are held on the paddle with two narrow strips of plastic wrapping. Eight of these paddles are placed under the upper window. To adapt the flat paddle to the round ACC window we use a foam core radius adapter. Through precision holes in the upper window the aerogel paddle and radius adapter are tied to the upper window. To insure light-tightness, the upper window is covered with an opaque layer of DuPont Tedlar. The counter has two blue LED for PMT calibration.

3. Testing and Flight Performance

We have tested the ACC PMT assemblies extensively prior to the selection of those to be used for flight. Each PMT assembly together with its associated HV supply underwent a 3-day thermal-vacuum test during which the PMT current, noise rate, and gain was tested at different HV settings. In addition, a prototype counter design was verified in a beam test at KEK, Japan. The HV for the PMTs is set so that all PMTs have nominally the same gain. The setting was later verified in the instrument, with the magnetic field on, using the LEDs.

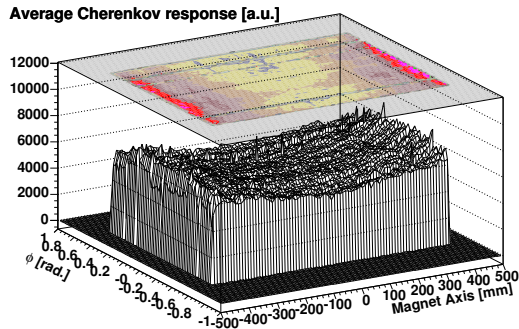


Figure 3. Response Map of the Aerogel Cherenkov Counter for relativistic protons.

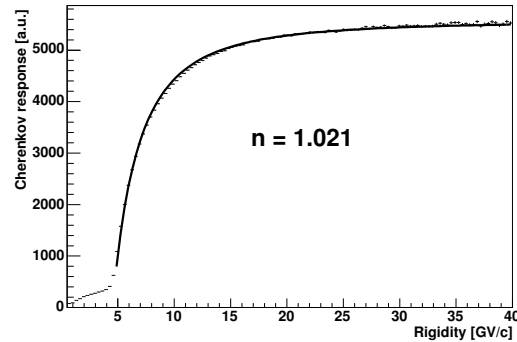


Figure 4. Average Cherenkov signal vs. Rigidity for proton flight data and fitted index-of-refraction, $n = 1.021$.

During flight, one PMT of 46 was turned off as a precaution, because this PMT had an indication of unstable current. The remaining PMTs worked as expected. During bench testing of the PMT and the flight HV supply, we noticed a broadening of the pedestal compared to the pedestal obtained with a highly filtered laboratory HV power supply. The sigma of the pedestal broadened by a factor of 5 to ~ 15 QDC channel per PMT when changed to the flight power supplies. Due to time constraints and the large number of channels involved, additional filtering of the HV was not possible for this flight.

We used in-flight proton data to calibrate the Cherenkov counter. In the further analysis we used the combined signal of all ACC PMTs. Figure 3 shows the average, path-length-corrected Cherenkov response for relativistic protons creating a saturated Cherenkov signal in the counter as a function of the particle position. This map shows a small dependence of the ACC signal on the azimuthal position. Along the axis of the magnet it varies from center the edge by 27%. Proton data was also used to determine the effective index-of-refraction for the counter. Figure 4 shows the average Cherenkov response in the fiducial volume versus the rigidity for protons. The solid line is Cherenkov response for the fitted index-of-refraction, which was found at, $n = 1.021$. Below the Cherenkov threshold there is a small signal possibly from Cherenkov light generated in the Gore-Tex reflector and light from δ -ray electrons above the aerogel threshold.

This Cherenkov counter is primarily used as threshold detector to suppress lighter particles. Of importance as a veto counter is its rejection power, which depends number of PEs. To determine a lower limit for the number of PEs, we fitted the distribution of the path-length-corrected ACC response for relativistic protons for each block. We obtained used a sigma-over-mean method 7 PEs in the center of the counter and 9 PEs at the ends.

4. Summary

The ACC functioned as expected during the first BESS-Polar flight. The concept of the hermetic PMT housing worked so well that we consider it for the TOF in the next flight as well. While sufficient for the antiproton study, the number of PEs reported here is lower than for the past BESS experiment, which is partly due to the lower PMT quantum-efficiency (QE) in BESS-Polar and the increase number of interfaces in the aerogel. While in the past the fiducial volume contained 12 blocks of four aerogel sheets, BESS-Polar has 72 blocks of 7 aerogel sheets in conjunction with a lower depth of light diffusion box in BESS-Polar. The investigation of the potential use of the ACC as a velocity is still underway.

5. Acknowledgements

We would like to thank the National Scientific Balloon Facility and the National Science Foundation for their support of the balloon expedition. We also thank GSFC, KEK, ISAS, and ICEPP for continuous support. BESS-Polar is supported by a NASA Grant RTOP-188-05-10-01 in the US and by KAKENHI (13001004) in Japan.

References

- [1] M. Nozaki et al., NIM B 214, 110, (2004).
T. Yoshida et al., Advances in Space Research, 33, 1755, (2004).
J.W. Mitchell et al., Proceedings of Space Parts 2003 (Washington), Nuclear Physics B, submitted.
- [2] T. Yoshida et al., 29th ICRC, Pune (2005) OG 1.1.
S. Matsuda et al., 29th ICRC, Pune (2005) OG 1.1.
- [3] M. Sasaki et al., 29th ICRC, Pune (2005) OG 1.5.
- [4] Y. Asaoka et al., NIM A 416, 236, (1998).